*Solar-Terrestrial Physics. 2023. Vol. 9. Iss. 4. P. 17–24. DOI: 10.12737/stp-94202302. © 2023 N.S. Meshalkina, A.T. Altyntsev. Published by INFRA-M Academic Publishing House*

UDC 523.9-7, 523.98
DOI: 10.12737/stp-94202302

Received June 14, 2023
Accepted September 14, 2023

# BRIGHT ULTRAVIOLET KNOTS AS POSSIBLE SOURCES OF COHERENT MICROWAVE RADIATION

**N.S. Meshalkina**
*Institute of Solar-Terrestrial Physics SB RAS, Irkutsk, Russia, nata@iszf.irk.ru*

**A.T. Altyntsev**
*Institute of Solar-Terrestrial Physics SB RAS, Irkutsk, Russia, altyntsev@iszf.irk.ru*

**Abstract.** A distinctive feature of the September 6, 2012 event was that sources of narrow-band (2–4 GHz) sub-second pulses (SSP) were observed in small areas of flare loops with so-called bright ultraviolet knots with high plasma density up to $10^{11}$ cm$^{-3}$. Time profiles of hard X-rays of the flare, although similar to microwave light curves, do not have structures corresponding to SSP. Analysis of microwave, X-ray, and ultraviolet data has shown that the observable pulses of microwave radiation with a narrow spectral band are coherent in nature and are generated by electrons with energies of several tens of kiloelectronvolt in bright knots at a double plasma frequency. The results of the observations suggest that the appearance of bright knots is associated with local processes of energy release due to interaction of flare loops.

**Keywords:** Sun, fine temporal structure, UV bright knots, microwave bursts, coherent emission.

## INTRODUCTION

Radio observations can provide unique information about acceleration of non-thermal electrons, which can significantly complement the X-ray and ultraviolet observations. For example, responses to low fluxes of non-thermal particles, unobservable with state-of-the-art X-ray telescopes, can be recorded under favorable conditions in the radio range. Of particular interest are intense pulses of narrow-band radio emission lasting for less than 1 s, which, in general, are superimposed on a burst of longer duration and are reflected in the spectrum as fine spectral structures.

The fine time structure of solar radiation has been studied for several decades since the time when regular observations combining high spatial and spectral resolution appeared [Benz, 1986]. Consistent observations in microwave and X-ray ranges have shown that to sub-second pulses (SSPs) generally corresponds an increase in hard X-ray activity, yet there is no pulse-to-pulse correspondence except for broadband SSPs. Broadband SSPs with a band of more than a dozen GHz are generated by intense electron fluxes with an energy of several hundred keV through the gyrosynchrotron mechanism [Altyntsev et al., 2019].

Narrow-band microwave bursts with an instantaneous spectrum width of less than 2 GHz can be generated in the case of an unstable velocity distribution function of non-thermal electrons, beam or cone [Benz, 1986]. Generating SSPs in the microwave range, in addition to the nonequilibrium population of non-thermal electrons that excites plasma oscillations, requires subsequent conversion of turbulence of longitudinal oscillations into transverse electromagnetic waves. The SSP duration can also decrease relative to hard X-ray pulses because of violation of the conditions for access of electromagnetic radiation to the observer at frequencies close to plasma ones. Despite the difficulties in detecting SSPs, discussed in detail in the reviews [Fleishman, Melnikov, 1998; Altyntsev et al., 2023], narrow-band SSPs are a unique sensitive indicator of the occurrence of accelerated particles in flare processes.

Altyntsev et al. [2023] have reviewed studies of bursts with the fine time structure in the microwave (centimeter) range (frequencies above 3 GHz) whose sources are located in the vicinity of the regions of primary energy release of solar flares, where electrons are accelerated, in low flare loops. At a frequency of 5.7 GHz belonging to this range, observations were carried out with the Siberian Solar Radio Telescope (SSRT) at high spatial and temporal resolution from 2000 to 2013. During this period, an archive containing more than 200 events with subsecond pulses was created. From 2010, the archive was supplemented with dynamic spectra obtained by the Badary Broadband Microwave Spectropolarimeter (BBMS) [https://badary.iszf.irk.ru/Ftevents.php]. SSPs are associated with flare activity of active regions, are generated by a coherent mechanism in a narrow frequency band (up to 2 GHz), and are quite rare: they were observed in ~10 % of bursts at 5.7 GHz [Zhdanov, Zandanov, 2015; Altyntsev et al., 2023].

The main reason for the rare observation of SSPs is absorption of their radiation in the vicinity of the source since the frequency of their radiation is close to the plasma frequency or its harmonic [Benz et al., 1992]. To detect SSPs at the SSRT receiving frequency of 5.7 GHz, the plasma density in the source should be as high as $10^{11}$ cm$^{-3}$ and decrease along the line of sight on a scale of no more than a thousand kilometers [Altyntsev et al., 2007]. It is therefore interesting to examine the relationship between the occurrence of narrow-band bursts of coherent emission with bright knots in flare loops visible in extreme ultraviolet (EUV) [Cheng,

1980; Widing, Hiei, 1984; Golub et al., 1999; Warren, 2000] and in soft X-rays [Lin et al., 1984; Shimizu et al. al., 1994; Doschek et al., 1995].

Doschek et al. [1995] have found compact regions of increased brightness at the tops of the loops visible in soft X-rays recorded by the Yohkoh satellite. Temperatures in them were as high as 7–20 MK; and electron densities, $10^{11}$–$10^{12}$ cm$^{-3}$. These bright knots accounted for 30 % of the emission of the total value.

Kołománski et al. [2017] with the aid of AIA/SDO have detected small-scale (several arcsec) hot (10 MK) sources of ultraviolet radiation at the top of a flare loop during the decaying phase of the flare. Modeling of X-rays from EUV data did not show the presence of compact sources.

Properties of bright EUV knots can be summarized as follows:

1) high temperature — from 1 to 10 MK;
2) compactness — the size does not exceed a few arcsec;
3) duration — the lifetime ranges from a few seconds to ten minutes;
4) intensity — the brightness of individual pixels can be several times higher than the average values in the neighborhood;
5) motion — velocities recorded are tens of kilometers per second;
6) high density — to $10^{11}$–$10^{12}$ cm$^{-3}$.

Two hypotheses on the formation of bright knots have been put forward. The first suggests that these fine-structured bright formations are related to small-scale reconnection events in low loops with scales below the TRACE or SXT/Yohkoh resolution [Tsuneta et al., 1991; Shimizu et al., 1994; Doschek et al., 1995; Warren, 2000]. The second hypothesis was proposed in [Patsourakos et al., 2004], in which TRACE observations of bright knots were analyzed [Handy et al., 1999] and their motion was detected. The authors assumed that the formation of knots is associated with the disbalance between heating and radiation cooling in local regions of magnetic loops.

We have analyzed in detail multi-wave observations of the September 6, 2012 solar flare. This event is unusual in that the fine time structure was observed during the main phase of the flare in which the so-called bright knots in flare loops were detected in several EUV channels of AIA/SDO. The purpose of this work is to examine the response in microwave radiation to bright knots visible in EUV.

## INSTRUMENTS AND METHODS

The Siberian Solar Radio Telescope recorded one-dimensional (1D) scans of the solar disk at a frequency of 5.7 GHz with a time resolution of 14 ms in the east–west (EW) and north–south (NS) arrays [Altyntsev et al., 2003; Meshalkina et al., 2012]. The SSRT antenna beamwidth was 22″ and 20″ in the EW and NS directions respectively. We used sequences of 1D SSRT scans to detect short radio bursts lasting for less than 1 s. The 1D scans were also employed to localize the SSP sources on the solar disk. SSRT also recorded two-dimensional (2D) solar disk images every 2-3 minutes [Grechnev et al., 2003; Kochanov et al., 2013]. The 2D images were used to study properties and location of the background source of the microwave burst during the flare.

To measure the spectrum, we utilized BBMS data [Zhdanov, Zandanov, 2011] in the 4–8 GHz frequency range with 10 ms time resolution. Sequences of images obtained by the Nobeyama Radioheliograph (NoRH) [Nakajima et al., 1994] at a frequency of 17 GHz were used to study spatial distribution of radio burst and radiation intensity variations with 10″ resolution. Light curves were measured by Nobeyama Radio Polarimeters (NoRP) [Torii et al., 1979] with 1 s resolution at frequencies of 1, 2, 3.75, 9.4, 17, 35 GHz.

We took data on spectral and spatial characteristics of EUV radiation from the Solar Dynamic Observatory (SDO) database [Pesnell et al., 2012]. We used full solar disk images with 0.6″ resolution recorded by AIA (Atmospheric Imaging Assembly)/SDO every 12 s [Lemen et al., 2012]. Six optically thin AIA/SDO EUV channels (171, 193, 211, 131, 335, and 094 Å) were exploited to calculate the emission measure at temperatures $5.5<\lg T<7.5$. The differential emission measure was calculated by the inversion method [Cheng et al., 2012].

Fermi Gamma-Ray Burst Monitor (Fermi/GBM) [Meegan et al., 2009] is an instrument aboard the Fermi Space Telescope [Atwood et al., 2009] that provides light curves in the spectral range from 8 keV to 40 MeV; the time resolution is 256/64 ms.

We have used RHESSI (Reuven Ramaty High Energy Solar Spectroscopic Image) data [Lin et al., 2002] for obtaining light curves with 100 ms time resolution in order to study the time structure of X-rays, as well as to construct images with 4 s resolution.

We have also employed data from RSTN (Radio Solar Telescope Network) [Guidice et al., 1981] consisting of four stations: in Learmont (Australia) (we use the data for our study), San Vito (Italy), Sagamore Hill (USA), and Palehua (USA), which measure the intensity at eight frequencies (245, 410, 610, 1415, 2695, 4995, 8800, and 15400 MHz) with 1 s resolution.

## OBSERVATIONS

The September 6, 2012 flare occurred in active region (AR) 1564 and lasted from 02:32 to 02:44 UT (UT); its class according to GOES is C2.4. During the flare main phase, a fine time structure was recorded by SSRT. Figure 1 shows light curves of the flare in soft X-rays and the dynamic spectra of microwave radiation. Figure 1, *b* represents the composite dynamic spectrum obtained from NoRP and BBMS data.

During the flare, two main broadband (from 2 to 16 GHz) bursts were observed with narrowband bursts with a spectrum width from 2 to 4 GHz between them (see Figure 1, *c*). We excluded the first short peak in Figure 1, *c* from consideration since it turned out to be longer than 1 s and was not narrowband: its width is more than 4 GHz, which is clearly visible in the spectrum. In this paper, we analyze subsecond bursts in a 30 s interval (02:36:40–02:37:10 UT), bounded by vertical dashed lines

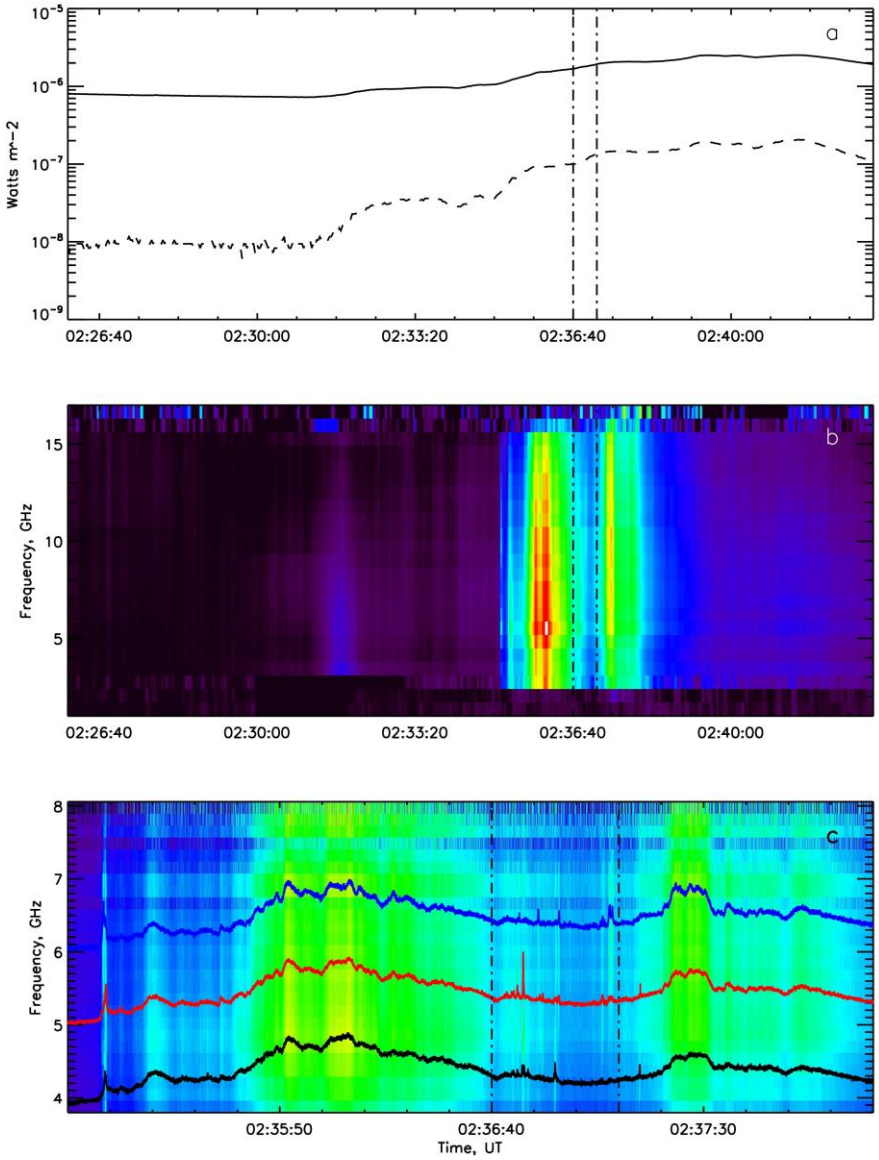


*Figure 1*. September 6, 2012 event: *a* — GOES data, radiation fluxes in 1–8 Å (solid curve) and 0.5–4 Å (dashed curve); *b* — composite dynamic spectrum in the microwave range from NoRP and BBMS data; *c* — BBMS dynamic spectrum with separately selected profiles (denoted by color) at frequencies of 4.07, 5.03, and 6.07 GHz. Vertical dash-dot lines mark the interval with a fine time structure

in the panels. In this interval at three frequencies, the radiation bandwidth of the subsecond bursts is comparable to the difference between their frequencies — ~2 GHz.

Figure 2, *a* displays time profiles at a frequency of 5.744 GHz with 10 ms resolution, obtained from the BBMS dynamic profile during the flare. There are two main bursts and a fine time structure between them. Figure 2, *b* demonstrates intensity profiles for the SSP interval with 14 ms time resolution, recorded by SSRT at 5.7 GHz.

Images of the energy release region and contours of flare sources are presented in Figure 3. The microwave radiation of the background burst at 5.7 GHz (white contours) covers bright EUV loops (131 Å). A compact radiation source at 17 GHz (pink contours) is located near the source brightness center at 5.7 GHz. Hard X-ray data in channels 6–12 keV (red contours) and 12–25 keV (purple contours) shows a large low loop oriented along an ensemble of EUV loops. Footpoints of the EUV loops are spaced in latitude and are located in the regions of small pores and sunspots of negative polarity in the east and positive polarity in the west (see Figure 3,*b*).

SSRT data allows us to localize the SSP sources relative to the brightness center of the background burst [Meshalkina et al., 2004]. In our event, the brightness centers of the SSP sources appeared in the region indicated by the blue frame in Figures 3, *b* and 4. To quantify the shift values, we used centroids of the scans. It can be seen (Figures 3, *a* and 4) that the SSP generation region is shifted from the center of the brightness of the background burst by ~10″ southwestward and is located at the tops of the loops visible in hard X-rays and EUV.

To analyze the spatial dynamics of bright knots during the flare (see Figure 4), we have identified four fragments of the image in the flare region.

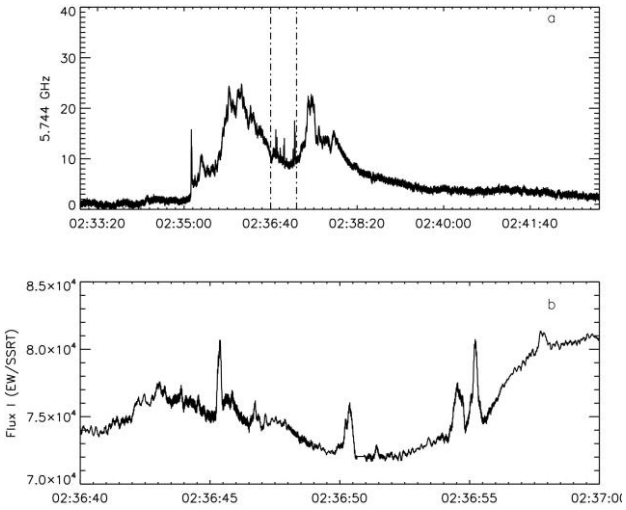


*Figure 2.* Time profile of the intensity at a frequency of 5.744 GHz, obtained from the BBMS dynamic profile; vertical dash-dot lines mark the interval with SSPs (*a*); time profiles of the radio emission flux in the time interval with SSPs, obtained by SSRT (*b*)

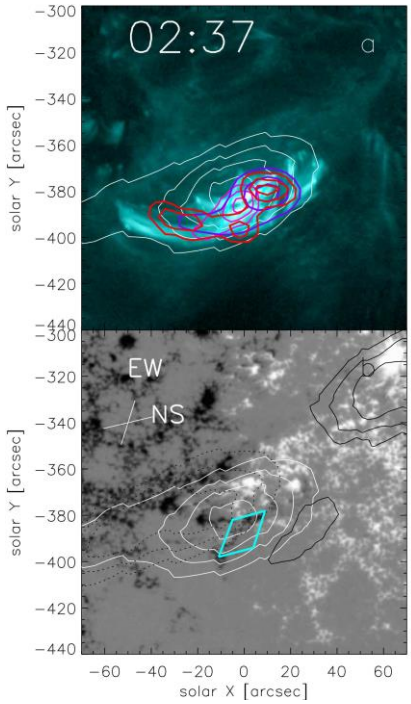


*Figure 3.* Image in the 131 Å channel (AIA/SDO) at 02:35:10 UT with superimposed contours (*a*): white contours — distribution of brightness temperature (image at 5.7 GHz at 02:37 UT) at levels 0.3, 0.5, 0.7, 0.9 from its maximum; pink — intensity distribution of brightness temperature (levels 0.5, 0.7, 0.9 from the maximum) at 17 GHz at 02:37; purple and red — RHESSI data in the 12–25 and 6–12 keV channels (levels 0.2, 0.5, 0.8 from the maximum) respectively. The blue frame in this and the next panels indicates the location of an SSP source. HMI/SDO magnetogram at 02:37:06 with superimposed contours (*b*): white contours — intensity distribution of brightness temperature (levels 0.3, 0.5, 0.7, 0.9 from the maximum) at 5.7 GHz (SSRT); black contours — distribution of brightness temperature in circular polarization at 5.7 GHz: solid contours— right polarization (levels 0.5, 0.7, 0.9 from the maximum); dotted contours — left polarization (levels 0.5, 0.7, 0.9 from the minimum). The white oblique cross in the top left corner is the SSRT antenna beam

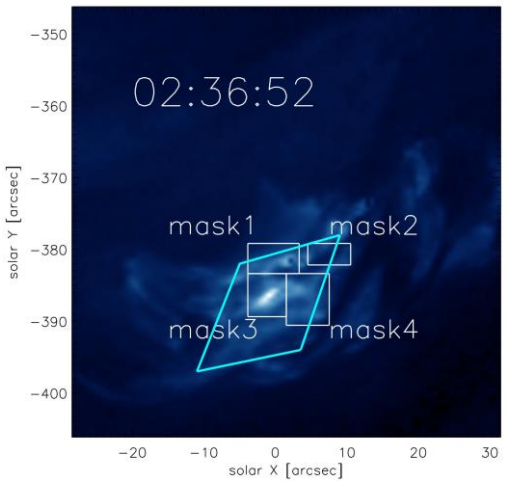


*Figure 4.* Bright knots according to AIA/SDO UV data in the 335 Å channel at 02:36:52 UT. The places where the SSP sources appeared are indicated by the blue frame (as in Figure 3)

It is noteworthy that the bright knots were observed in different AIA/SDO channels (171, 193, 304 Å). Image sequences in the 171 Å line, which corresponds to the 0.6 MK temperature of active regions in the corona, are displayed in Figure 5. In the images there are bright points to 5″ in size.

The dynamics of bright knots throughout the flare in EUV in the 335 Å channel (AIA/SDO) is presented in the movie [http://ru.iszf.irk.ru/~nata/120906/335_blue.mp4]. Figure 4 shows that the region with SSP sources covers all four selected fragments. Bright knots alternately appear and disappear inside these fragments, move in different directions. The possibilities of tracking the motion of bright knots are limited by the 12 s time resolution of the EUV images.

Figure 6 illustrates the time variation in the 335 Å integral UV flux calculated from four fragments. The well-defined increase in the flux in the second and third fragments corresponds in time to the interval with SSPs. There is no such unambiguous correspondence for the remaining fragments.

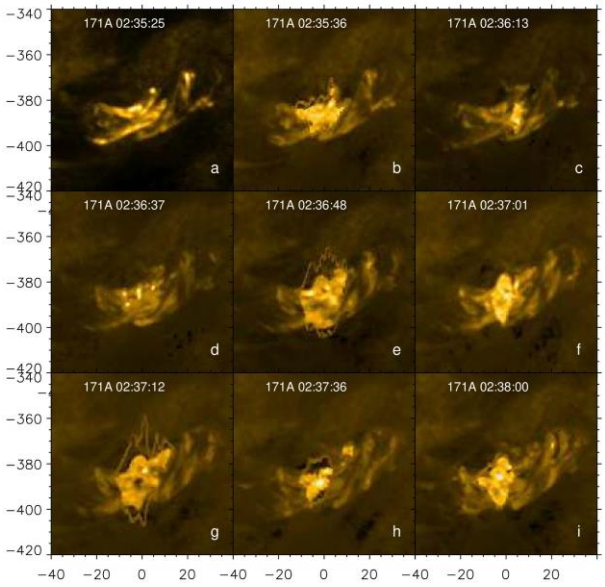


*Figure 5.* Bright knots according to AIA/SDO UV data in the 171 Å channel throughout the flare; *e* and *f* are images during SSP

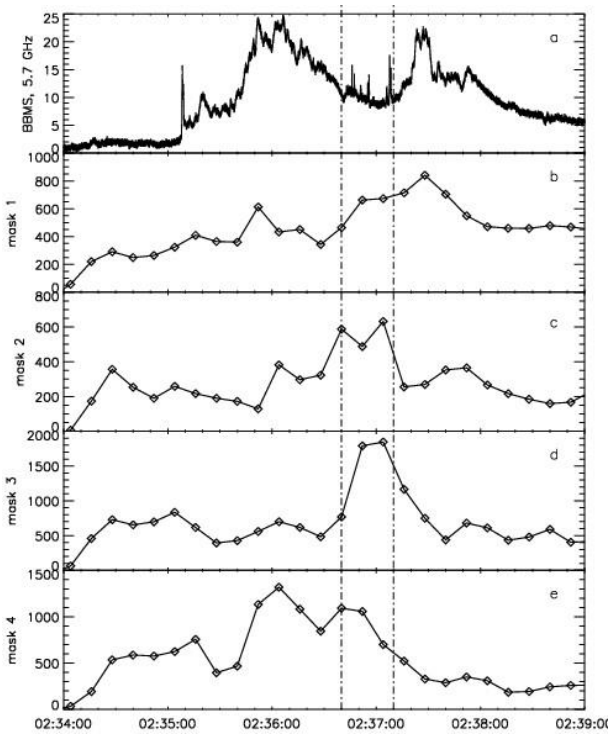


*Figure 6.* Time profiles of the 335 Å EUV radiation flux calculated from four fragments in Figure 4

Figure 7 exhibits time profiles in radio and X-ray radiation.

In the 25–50 keV Fermi channel with 64 ms resolution, we can see short pulses; RHESSI data with 100 ms time resolution no longer shows the fine structure, but demonstrates only two main bursts due to low sensitivity. When observing an SSP group detected in radio emission, we do not observe a response in X-rays at both instruments. In Figure 7, d, e, there are two main broadband bursts of incoherent nature in radio emission.

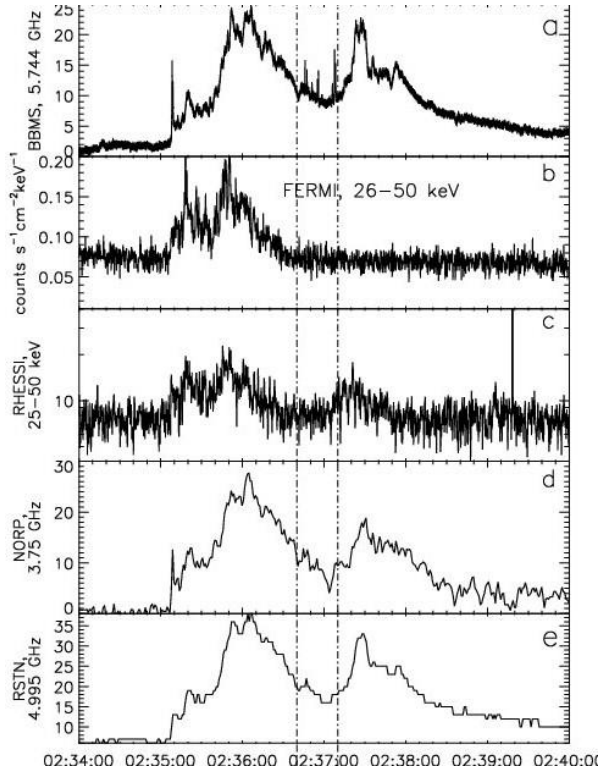


*Figure 7.* Time profiles in microwave and hard X-ray radiation: data from BBMS at 5.744 GHz (*a*), Fermi/GBM (*b*), RHESSI 25–50 keV (*c*), NoRP (*d*), and RSTN (*e*)

## DISCUSSION

In Figure 1 in the spectrum, obtained by BBMS, and time profiles, the fine time structure is observed on the interval between two main bursts visible in radio and hard X-ray ranges. The bandwidth of the spectrum of these SSPs ranges from 2 to 4 GHz. Unlike bursts with a bandwidth of >4 GHz, narrow-band SSPs are generated by a coherent mechanism. We have previously shown that the coherent microwave radiation at SSRT receiving frequencies is generated by electrons with energies of several tens of kiloelectronvolt through plasma mechanisms near double Langmuir frequency ([Altyntsev et al., 2023] and references therein).

The SSRT observations suggest that narrow-band subsecond bursts are generated in the region of flare loops, in which bright EUV knots occurred at that time. In order for them to be sources of plasma radiation at 5.7 GHz, the plasma density in them should be as high as $10^{11}$ cm$^{-3}$.

The plasma density can be estimated using a measure of ultraviolet radiation $EM = \int DEM\left(T_{\log}\right) dT_{\log}$, where *DEM* is the differential emission measure, $T_{\log}$=lg(*T*). The differential emission measure and the solution error have been obtained by the inversion method [Cheng et al., 2012]; measurement units [cm$^{-5}$ K$^{-1}$]. The input data are SDO/AIA images in ultraviolet radiation in six channels (94, 131, 171, 193, 211, and 335 Å) for 02:37 UT. At that time, the temperature dependence of *DEM* had one maximum at low temperatures of 0.3 MK (which corresponds to the peak of radiative losses of

optically thin plasma) and the second wide maximum at $T$≈2.5 MK (Figure 8). The electron density can be estimated as $n_e = \sqrt{EM / l}$, where $l$ is the thickness of the emission region along the line of sight. Near the bright point (in Figure 9, it is indicated by a white frame) at $l$=1.74×10$^8$ cm (the transverse size of the bright knot is four pixels, an AIA pixel is 0.6″), we have detected the maximum density $n_e$≈9×10$^{10}$ cm$^{-3}$. Thus, the plasma density in the source is sufficient to generate the harmonic of plasma frequency in a knot. The mechanism of electromagnetic wave generation at a frequency near the double plasma one has been examined in many works (see, e.g., [Benz et al., 1992]). Outside the knot, the plasma density decreases sharply — several times at distances of ~1 arcsec, which, firstly, limits the SSP source at 5.7 GHz to the size of the bright EUV knot and, secondly, creates favorable conditions for the SSP radiation to escape from the bright knot.

Collisional absorption in the lower corona significantly affects the observation of microwave SSPs. Benz et al. [1992] have concluded that in the case of a magnetic flux tube filled with dense plasma, the SSP radiation can be observed if it reaches the observer across the magnetic tube and the negative plasma density gradient in this direction is large enough. We have previously shown [Meshalkina et al., 2004] that SSP sources are observed more often at the tops of loops when radiation escapes across a loop.

When emitted at a frequency close to the double Langmuir one, the required plasma density is four times lower (at 5.7 GHz, the density in a flare loop is 10$^{11}$ cm$^{-3}$) than for the fundamental frequency. In this case, absorption in the plasma surrounding the source decreases by an order of magnitude. Absorption during emission of the second plasma frequency harmonic is estimated in [Benz et al., 1992]:

$$\tau = \begin{Bmatrix} 46 \\ 1.2 \end{Bmatrix} T^{-3/2} \nu^2 H_r, \qquad (1)$$

where T is the temperature in a loop [K]; v is the frequency [GHz]; Hr is the scale of density variation [cm]. In our case, at 5.7 GHz and T=2.5 MK, we get Hr=1000 km. Thus, the conditions for radiation escape for knots with sizes of several arcsec are met.

The relatively high temperature and the plasma density increased relative to the environment, as well as the

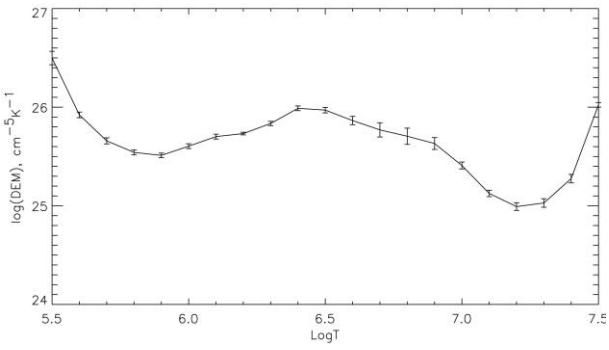


*Figure 8*. Differential emission measure calculated for 02:37 UT. Measurement errors (three standard deviations) are marked with bars

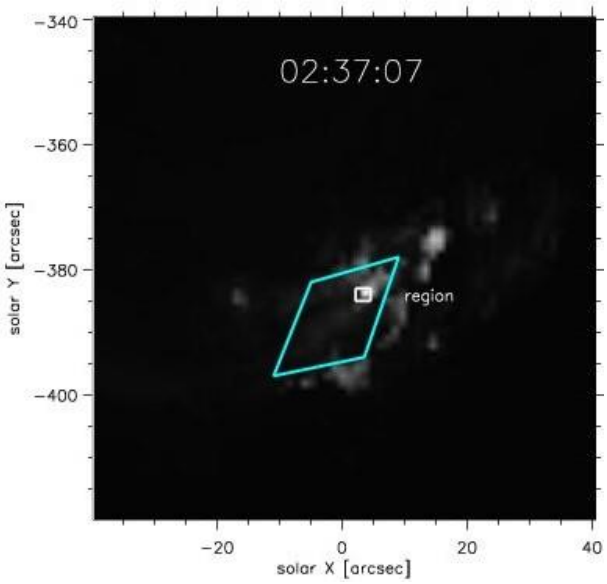


*Figure 9*. Background is the emission measure. The white frame marks the region in which the electron density was estimated. The blue frame, as in Figures 3, 4, indicates the location of SSP

presence of non-thermal electrons generating plasma radiation, argue for the interpretation of bright ultraviolet knots as sources of energy release. Such a scenario for the formation of bright knots has been proposed in [Tsuneta et al., 1991; Shimizu et al., 1994; Doschek et al., 1995; Warren, 2000]. Note that we have previously suggested that SSP sources are located in the region of primary energy release of solar flares [Altyntsev et al., 2023] (see also references therein).

## CONCLUSION

In the September 06, 2012 flare, a fine time structure was observed during the appearance of moving bright UV knots. SSP sources were seen in bright dense (10$^{11}$ cm$^{-3}$) and compact (3–5″) ultraviolet knots of coronal loops, which provided favorable conditions for plasma radiation escape in the microwave range observed at SSRT. The occurrence of pulses of non-thermal electrons indicates that bright knots are places of rapid energy release.

The X-ray data showed a correlation with microwaves only for two main bursts and did not demonstrate a response to the fine structure during the flare due to different mechanisms of radio and X-ray radiation, as well as possibly due to low sensitivity and insufficient time resolution of the Fermi and RHESSI X-ray telescopes. It is the observations of coherent microwave radiation that have a high diagnostic potential for detecting accelerating processes in small flares.

We are grateful to the anonymous reviewer and Yu.T. Tsap for the comments that significantly improved the article. The work was financially supported by the Ministry of Science and Higher Education of the Russian Federation. We are grateful to D.A. Zhdanov for his help in preparing BBMS data. We also thank the teams of the Solar Dynamic Observatory, GOES, the

Nobeyama Observatory, RHESSI, Fermi, RSTN, and the ISTP SB RAS Radio Astrophysical Observatory for providing data. The results were obtained using the Unique Scientific Facility "Siberian Solar Radio Telescope" [http://ckp-rf.ru/usu/73606/] and the equipment of Shared Equipment Center "Angara" [http://ckp-angara.iszf.irk.ru/].

## REFERENCES

Altyntsev A.T., Kuznetsov A.A., Meshalkina N.S., Yihua Y. On the origin of microwave type U-bursts. *Astronomy and Astrophysics*. 2003, vol. 411, p. 263. DOI: 10.1051/0004-6361:20031273.

Altyntsev A.T., Grechnev V.V., Meshalkina N.S., Yihua Y. Microwave type III-like bursts as possible signatures of magnetic reconnection. *Solar Phys.* 2007, vol. 242, iss.1-2, pp. 111–123. DOI: 10.1007/s11207-007-0207-9.

Altyntsev A.T., Meshalkina N.S., Lysenko A.L., Fleishman G.D. Rapid variability in the SOL2011-08-04 flare: Implications for electron acceleration. *Astrophys. J.* 2019, vol. 883, 338. DOI: 10.3847/1538-4357/ab3808.

Altyntsev A.T., Meshalkina N.S., Lesovoi S.V., Zhdanov D.A. Subsecond pulses in microwave emission of the Sun. *Physics-Uspekhi*. 2023, vol. 66, no. 7, pp. 691–703. DOI: 10.3367/UFNe.2022.06.039205.

Atwood W.B., Abdo A.A., Ackermann M., Althouse W., Anderson B., Axelsson M., et al. The Large Area Telescope on the Fermi Gamma-Ray Space Telescope Mission.*Astrophys. J.* 2009, vol. 697, pp. 1071–1102. DOI: 10.1088/0004-637X/697/2/1071.

Benz A.O. Millisecond Radio Spikes. *Solar Phys.* 1986, vol. 104, no. 1, pp. 99–110. DOI: 10.1007/BF00159950.

Benz A.O., Magun A., Stehling W., Su H. Electron beams in the low corona. *Solar Phys.* 1992, vol. 141, pp. 335–346. DOI: 10.1007/BF00155184.

Cheng C.C. Spatial distribution of XUV emission and density in a loop prominence. *Solar Phys*. 1980, vol. 65, iss. 2, pp. 347–356. DOI: 10.1007/BF00152798.

Cheng X., Zhang J., Saar S.H., Ding M.D. Differential emission measure analysis of multiple structural components of coronal mass ejections in the inner corona. *Astrophys. J.* 2012, vol. 761, 62. DOI: 10.1088/0004-637X/761/1/62.

Doschek G.A., Strong K.T., Tsuneta S. The bright knots at the tops of soft X-ray loops: Quantitative results from YOHKOH. *Astrophys. J*. 1995, vol. 440, p. 370. DOI: 10.1086/175279.

Fleishman G.D., Melnikov V.F. Millisecond solar radio spikes. *Physics-Uspekhi.* 1998, vol. 41, no. 12, pp. 1157–1189. DOI: 10.070/PU1998v041n12ABEH000510.

Grechnev V.V., Lesovoi S.V., Smolkov G.Ya., Krissinel B.B., Zandanov V.G., Altyntsev A.T., et al. The Siberian Solar Radio Telescope: the current state of the instrument, observations, and data. *Solar Phys*. 2003, vol. 216, pp. 239–272. DOI: 10.1023/A:1026153410061.

Golub L., Bookbinder J., DeLuca E., Warren H., Schrijver C.J., Shine R., et al. A new view of the solar corona from the transition region and coronal explorer (TRACE). *Physics of Plasmas*. 1999, vol. 6, iss. 5, pp. 2205–2216. DOI: 10.1063/1.873473.

Guidice D.A., Cliver E.W., Barron W.R., Kahler S. The Air Force RSTN System. *Bull. of the American Astronomical Soc*. 1981, vol. 13, p. 553.

Handy B.N., Acton LW., Kankelborg C.C., Wolfson C.J., Akin D.J., Bruner M.E., et al. The Transition Region and Coronal Explorer. *Solar Phys*. 1999, vol. 187, pp. 229–260. DOI: 10.1023/A:1005166902804.

Kochanov A.A., Anfinogentov S.A., Prosovetsky D.V., Rudenko G.V., Grechnev V.V. Imaging of the solar atmosphere by the Siberian Solar Radio Telescope at 5.7 GHz with an enhanced dynamic range. *Publ. Astron. Soc. Japan.* 2013, vol. 65, no. SP1, article id. S19. DOI: 10.1093/pasj/65.sp1.S19.

Kolomanski S., Mrozek T., Chmielewska E. Fine structure and long duration of a flare coronal X-ray source with RHESSI and SDO/AIA data. *arXiv:1701.09127*. 2017. DOI: 10.48550/arXiv.1701.09127.

Lemen J.R., Title A.M., Akin D.J., Boerner P.F., Chou C., Drake J.F., et al. The Atmospheric Imaging Assembly (AIA) on the Solar Dynamics Observatory (SDO). *Solar Phys*. 2012, vol. 275, no. 1-2, pp. 17–40. DOI: 10.1007/s11207-011-9776-8.

Lin R.P., Schwartz R.A., Kane S.R., Pelling R.M., Hurley K.C. Solar hard X-ray microflares. *Astrophys. J.* 1984, vol. 283, pp. 421─425. DOI: 10.1086/162321.

Lin R.P., Dennis B.R., Hurford G.J., Smith D.M., Zehnder A., Harvey P.R., et al. The Reuven Ramaty High-Energy Solar Spectroscopic Imager (RHESSI). *Solar Phys*. 2002, vol. 210, pp. 3–32. DOI: 10.1023/A:1022428818870.

Meegan C., Lichti G., Bhat P.N., Bissaldi E., Briggs M.S., Connaughton V., et al. The Fermi Gamma-ray Burst Monitor. *Astrophys. J.* 2009, vol. 702, pp. 791–804. DOI: 10.1088/0004637X/702/1/791,

Meshalkina N.S., Altyntsev A.T., Sych R.A., Chernov G.P., Yihua Y. On the wave mode of subsecond pulses in the cm-range. *Solar Phys.* 2004, vol. 221, pp. 85–99. DOI: 10.1023/B:SOLA.0000033356.96547.65.

Meshalkina N.S., Altyntsev A.T., Zhdanov D.A. Study of flare energy release using events with numerous type III-like bursts in microwaves.*Solar Phys.* 2012, vol. 280, no. 2, p. 537. DOI: 10.1007/s11207-012-0065-y.

Nakajima H., Nishio M., Enome S., Shibasaki K., Takano T., HanaokaY., et al. The Nobeyama Radioheliograph. *Proc. IEEE*. 1994, vol. 82, no. 5, pp. 705–713.

Patsourakos S., Antiochos S.K., Klimchuk J.A. A model for bright extreme-ultraviolet knots in solar flare loops. *Astrophys. J*. 2004, vol. 614, iss. 2, p. 1022. DOI: 10.1086/423779.

Pesnell W.D., Thompson B.J., Chamberlin P.C. The Solar Dynamics Observatory (SDO). *Solar Phys*. 2012, vol. 275, iss. 1-2, pp. 3–15. DOI: 10.1007/s11207-011-9841-3.

Shimizu T., Tsuneta S., Acton L.W., Lemen J.R., Ogawara Y., Uchida Y. Morphology of active region transient brightenings with the YOHKOH Soft X-Ray Telescope. *Astrophys. J.* 1994, vol. 422, pp. 906–911. DOI: 10.1086/173782.

Torii C., Tsukiji Y., Kobayashi S., Yoshimi N., Tanaka H., Enome S. Full-automatic radiopolarimeters for solar patrol at microwave frequencies. *Proc. of the Research Institute of Atmospherics*, Nagoya University, 1979, vol. 26, pp. 129–132.

Tsuneta S., Acton L., Bruner M., Lemen J., Brown W., Caravalho R., et al. The Soft X-ray Telescope for the SOLAR-A mission. *Solar Phys.* 1991, vol. 136, pp. 37–67. DOI: 10.1007/BF00151694.

Widing K., Hiei E. A SKYLAB flare associated with a hard X-ray burst. *Astrophys. J*. 1984, vol. 281, p. 426. DOI: 10.1086/162113.

Warren H.P. Fine structure in solar flares. *Astrophys. J.* Vol. 536, iss. 2, pp. L105–L108. DOI: 10.1086/312734.

Zhdanov D.A., Zandanov V.G. Broadband microwave spectropolarimeter. *Central European Astrophysical Bulletin*. 2011, vol. 35, p. 223.

Zhdanov D.A., Zandanov V.G. Observations of microwave fine structures by the Badary Broadband Microwave Spectropolarimeter and the Siberian Solar Radio Telescope. *Solar Phys.* 2015, vol. 290, no. 1, p. 287. DOI: 10.1007/s11207-014-0553-3.

URL: https://badary.iszf.irk.ru/Ftevents.php (accessed June 2, 2023).

URL: http://ru.iszf.irk.ru/~nata/120906/335_blue.mp4 (accessed June 2, 2023).

URL: http://ckp-rf.ru/usu/73606/ (accessed June 2, 2023).

URL: http://ckp-angara.iszf.irk.ru/ (accessed June 2, 2023).

Original Russian version: Meshalkina N.S., Altyntsev A.T., published in Solnechno-zemnaya fizika. 2023. Vol. 9. Iss. 4. P. 21–29. DOI: 10.12737/szf-94202302. 

*How to cite this article*

Meshalkina N.S., Altyntsev A.T. Bright ultraviolet knots as possible sources of coherent microwave radiation. *Solar-Terrestrial Physics*. 2023. Vol. 9. Iss. 4. P. 17–24. DOI: 10.12737/stp-94202302.